

# Negative DC Prebreakdown Phenomena and Breakdown-Voltage Characteristics of Pressurized Carbon Dioxide up to Supercritical Conditions

Tsuyoshi Kiyam, *Member, IEEE*, Akihiro Uemura, Bhupesh C. Roy, Takao Namihira, *Senior Member, IEEE*, Masanori Hara, *Fellow, IEEE*, Mitsuru Sasaki, Motonobu Goto, and Hidenori Akiyama, *Fellow, IEEE*

**Abstract**—This paper deals with the experimental results on prebreakdown phenomena and breakdown voltage characteristics of a negative dc point-to-plane gap in-compressed carbon dioxide up to the supercritical pressure as the first step to develop a plasma reactor with supercritical carbon dioxide. The gap length and the curvature radius of the point tip were 200 and around 35  $\mu\text{m}$ , respectively. The experimental results show the following: 1) corona discharge preceding complete breakdown is observed more clearly in liquid and supercritical fluid than in gas; 2) the estimated discharge onset voltage according to the streamer theory is in fairly good agreement with the measured breakdown voltage in the gas density region of 0.1–30  $\text{kg} \cdot \text{m}^{-3}$ ; 3) the breakdown mechanism in liquid can be classified into two categories: bubble-triggered breakdown at lower pressure and non bubble-triggered breakdown at higher pressure; 4) the breakdown mechanism in supercritical fluid is similar to that in higher pressured liquid; and 5) the density and temperature dependences of breakdown voltage in liquid and supercritical fluid are related closely with the breakdown mechanism.

**Index Terms**—Bubble-triggered breakdown mechanism, corona discharge, electrical breakdown, plasma reactor, supercritical carbon dioxide (SC CO<sub>2</sub>).

## I. INTRODUCTION

**S**UPERCritical carbon dioxide (SC CO<sub>2</sub>) has recently become an attractive fluid for a variety of potential applications such as solvent-free reactions and thermolysis of organic system waste in chemical fields [1], [2], extraction of a useful ingredient and removal of toxic components in medical, pharmaceutical, and food processing fields [3]–[5], and a refrigerant for a heat pump in an air conditioner in a thermodynamic field [6], [7]. This is because of its unique characteristics such as high solubility, low viscosity, high diffusivity, nontoxic, nonflammable, and low critical temperature of 304 K [8], [9]. On the other hand, an electric discharge plasma has higher

chemical reactivity as well as benign properties for a global environment [10]. Therefore, the combination of SC CO<sub>2</sub> and an electrical discharge plasma may offer the possibility of a new horizon in future reaction fields.

Knowledge of the prebreakdown phenomena and breakdown characteristics of pressurized CO<sub>2</sub> up to supercritical conditions is required in order to develop a plasma reactor using SC CO<sub>2</sub>. With respect to the electrical discharge phenomena in SC CO<sub>2</sub>, Ito *et al.* [11], [12] measured dc breakdown voltages in SC CO<sub>2</sub> with a gap of tungsten coplanar film electrodes with a gap length of  $\mu\text{m}$ -order, which was produced using lithography and found the existence of a local minimum in the characteristics of breakdown voltage versus pressure. They presumed that the cause of the drastic decrease in breakdown voltage near the critical point is electron attachment to existing clusters in dense CO<sub>2</sub>. Recently, Lock *et al.* [13] studied experimentally the breakdown phenomena for a wire in a cylinder with an 84- $\mu\text{m}$  gap length in SC CO<sub>2</sub> using a pulse voltage of 100-ns duration and 10-ns rise time and reported that the breakdown voltage is three times lower than the Paschen's law estimations due to the inhomogeneity of the CO<sub>2</sub> density near the critical point. On the other hand, in order to develop gases and gas mixtures superior to pure SF<sub>6</sub>, which has excellent dielectric properties but a weak point of high global warming potential, dc breakdown voltages of CO<sub>2</sub> gas pressurized up to 1.5 MPa have been measured [14]. Unfortunately, several aspects of the breakdown mechanism and characteristics in pressurized CO<sub>2</sub> up to the supercritical pressure still remain incomplete.

This paper deals with prebreakdown phenomena and breakdown voltage characteristics of a negative dc point-to-plane gap in compressed CO<sub>2</sub> up to the supercritical pressure as the first step to develop a plasma reactor with SC CO<sub>2</sub>.

## II. EXPERIMENTAL SETUP AND METHOD

### A. Thermodynamic State of CO<sub>2</sub> and Experimental Conditions

The thermodynamic state of CO<sub>2</sub> can be expressed by the combination of two state parameters such as temperature  $T$  and pressure  $P$  or density  $\rho$  and pressure. The ionization phenomena in gas, liquid, and supercritical fluids are dominated by the electron energy which is determined by the mean free path under a given electric field. Therefore, it is desirable to choose the density as one of two parameters to express the state

Manuscript received December 3, 2006; revised March 8, 2007. This work was supported in part by Grants-in-Aid for Scientific Research (A) under Grant 17206080 from the Japan Society for Promotion Science, and the 21st Century Center of Excellence Program on Pulsed Power Science under Grant 50015903 from the Ministry of Education, Culture, Sports, Science, and Technology.

The authors are with the Graduate School of Science and Technology, Kumamoto University, Kumamoto 860-8555, Japan (e-mail: kyan@sci.kumamoto-u.ac.jp).

Color versions of one or more of the figures in this paper are available online at <http://ieeexplore.ieee.org>.

Digital Object Identifier 10.1109/TPS.2007.896774

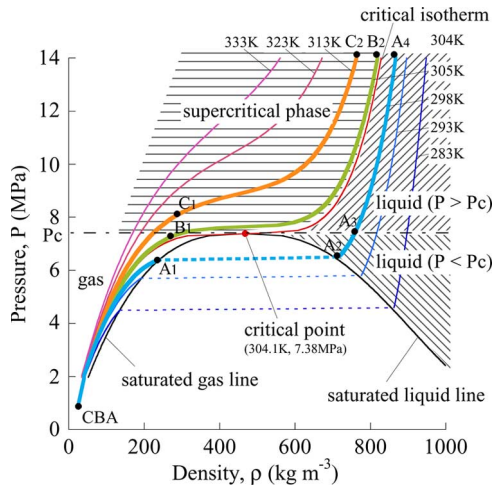


Fig. 1. Regions of carbon dioxide pressure–density diagram.

of the tested CO<sub>2</sub> since the density varies inversely as the mean free path.

Fig. 1 shows the density versus pressure relation for CO<sub>2</sub> as a parameter of temperature [15]. The critical point is at  $T_c = 304.1$  K and  $P_c = 7.38$  MPa. Obviously, the state of CO<sub>2</sub> is categorized into the three states of gas, liquid, and supercritical fluid, as shown in the figure. For convenience in later discussions, the liquid state was divided into two regions of higher and lower pressures than the  $P_c$ . They are called “lower pressurized liquid” and “higher pressurized liquid” in the paper, respectively. In the present experiments, the temperature was set first, and the pressure was decreased from supercritical to atmospheric pressure during the observation of the prebreakdown phenomena. The chosen temperatures of 298, 305 and 313 K as the basic temperature conditions are illustrated by three thick-solid lines, A – A<sub>1</sub> – A<sub>2</sub> – A<sub>3</sub> – A<sub>4</sub>, B – B<sub>1</sub> – B<sub>2</sub> and C – C<sub>1</sub> – C<sub>2</sub> in the figure. These lines correspond to normal, near critical, and supercritical temperatures, respectively, and the change of CO<sub>2</sub> state along the lines differs by temperature.

### B. Experimental Apparatus and Method

The electrode system was set in a chamber which will be used as the test reactor for plasma production in the future. The schematic diagram of the experimental set up is shown in Fig. 2(a). The test chamber with a bore of 105 mm and length of 100 mm was made of SUS316 stainless steel and is able to hold pressures up to 30 MPa. It was sealed with a double O-ring. The power lead was fed through a special design high-voltage bushing of polyetheretherketone resin into the test cell and was sealed with a double O-ring.

A point-to-plane gap geometry with 200- $\mu$ m gap width  $d$  was chosen as the test gap since it is more convenient to study prebreakdown phenomena compared with that in a uniform field gap. The measured curvature radius of the point tip  $r$  was in the range of 30–40  $\mu$ m. The point electrode was made of tungsten to limit erosion from the arc at breakdown. The plane electrode was made of stainless steel. Assuming that the point electrode is a hyperbolic shape with the tip radius of

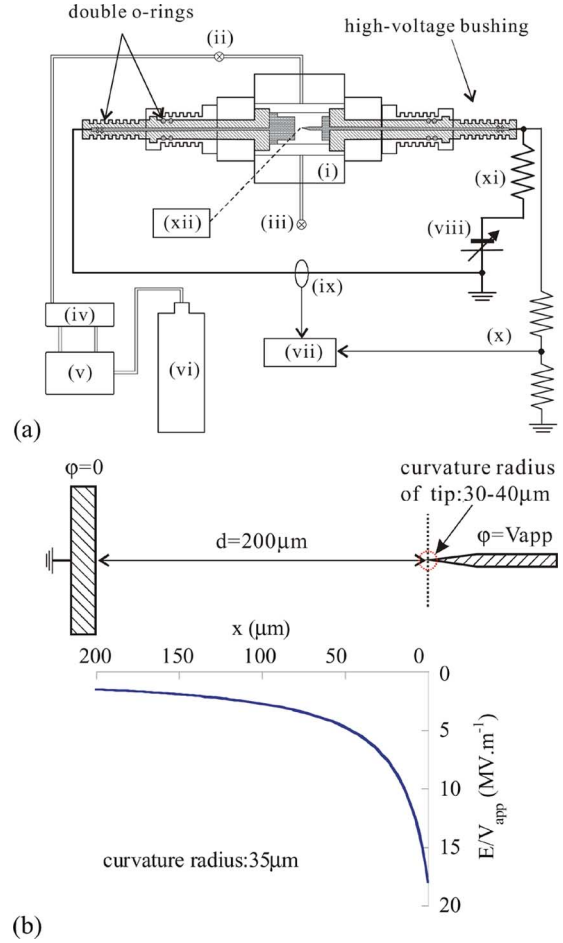


Fig. 2. Experimental setup and field distribution in the tested gap. (a) Schematic diagram of the experimental setup: (i) Test cell, (ii) CO<sub>2</sub> inlet, (iii) CO<sub>2</sub> outlet, (iv) syringe pump, (v) cooling system, (vi) CO<sub>2</sub> container, (vii) digital oscilloscope, (viii) dc power source, (ix) current transformer, (x) high-voltage probe, (xi) damping resistance, 2 M $\Omega$ , and (xii) PM. (b) Calculated field distribution in tested point-to-plane gap with curvature radius of tip 35  $\mu$ m.

35  $\mu$ m, the field distribution along the gap axis was calculated according to

$$E = \frac{2V_{\text{app}}}{(r + 2x) \ln(4d/r)} \quad (1)$$

where  $V_{\text{app}}$  is the applied voltage, and  $x$  is the distance from the point tip along the gap axis. Equation (1), as shown in Fig. 2(b), will be used to estimate the discharge onset voltage in the gas phase.

A dc power source with a rated current of 0.6 mA was connected to the point electrode through a 2-M $\Omega$  damping resistance to restrict the erosion of the point electrode by the discharge. Since the voltage drop on the damping resistance before complete breakdown was negligible, the supplied voltage may be applied fully to the tested gap. After the test cell was evacuated, liquid CO<sub>2</sub> was transferred from a CO<sub>2</sub> container to the test cell with a high-pressure pump. The temperature and pressure inside the test cell was controlled by a heater installed outside of the chamber and a backpressure regulator, respectively. After setting the wall temperature of the test cell

for a desired value, it took about 20 h to balance the temperature of the test chamber wall with that of the tested  $\text{CO}_2$ .

A series of experiments of prebreakdown observation and breakdown voltage measurement was done by changing pressure from higher pressure (14 MPa) to lower pressure (0.1 MPa) at the three desired temperatures, which were shown in Fig. 1 by the thick solid lines stated previously. After attaining the steady state condition of  $\text{CO}_2$ , the dc negative voltage was applied to the point electrode and increased at a rate of 2.5 kV/s by using a function generator (SG-4115, Iwatsu, Japan) and an amplifier (HAR-50R0.6, Matsusada Precision Inc., Japan). The time interval between successive voltage applications was at least 2 min to allow a steady state of the  $\text{CO}_2$  medium in which the density inhomogeneity and turbulence generated by the preceding breakdown may be minimized. Although the discharge current, discharge light, and acoustic emission were detected as indicators of corona discharge, the light measurement through the observation window of a chamber by a photomultiplier (PM) (No. 722, Atago Bussan Co. Ltd., Japan) gave the highest sensitivity. The PM signal and applied voltage were measured simultaneously with an oscilloscope.

### III. RESULTS AND DISCUSSION

#### A. Prebreakdown Phenomena

The corona light intensity  $I_{ph}$  and applied voltage  $V_{app}$  were recorded simultaneously to measure the corona onset and breakdown voltages, as shown in Fig. 3. These were obtained by additional experiments using a short gap of 80  $\mu\text{m}$  and a higher rate of voltage increase to show  $I_{ph}$  and  $V_{app}$  from corona initiation to complete breakdown. Because the sensitivity of PM was increased, the oscillogram shows the superposition of the thermal white noise on the light signal which was illustrated by the solid line on the trace.

The solid line on the light trace starts to rise at a critical voltage  $V_C$  and jumps suddenly until saturation of the PM output when the applied voltage collapses at  $V_B$ . Here,  $V_C$  and  $V_B$  are defined as corona onset and breakdown voltages, respectively. In the gas phase, the corona discharge is unstable, and weak corona light is often recognized just prior to breakdown, as shown in Fig. 3(a). In the liquid and supercritical phases, a corona discharge initiates well before breakdown, and the light intensity increases gradually with the applied voltage, as shown in Fig. 3(b) and (c). The corona onset voltages were almost the same for similar measurements of the medium state between liquid and supercritical phases.

#### B. Breakdown Voltage

1) *Density Dependency*: As stated before, the three chosen temperatures are normal, near critical, and supercritical temperatures, respectively, and the change of the  $\text{CO}_2$  state with the increase of density depends on the temperature, as shown in Fig. 1: at normal temperature of 298 K, via gas, lower and higher pressured liquids as indicated by the line A – A<sub>1</sub> – A<sub>2</sub> – A<sub>3</sub> – A<sub>4</sub>; at near critical temperature of 305 K, via gas and supercritical fluid as the line B – B<sub>1</sub> – B<sub>2</sub>; at

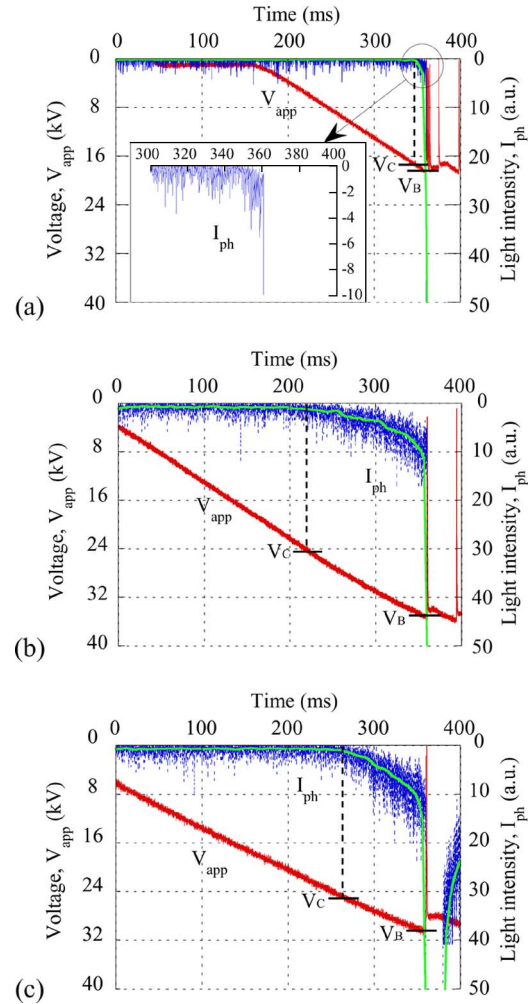


Fig. 3. Negative corona onset and breakdown voltages of three phases. (a) Gas phase. (b) Liquid phase. (c) Supercritical phase.

supercritical temperature of 313 K, via gas and supercritical fluid as the line C – C<sub>1</sub> – C<sub>2</sub>.

In Fig. 4, the average of four to five measured breakdown voltages and their deviation at the given conditions are illustrated by an open circle and a vertical bar as a function of the density. The density was estimated from the experimental condition of the temperature and pressure by using the equation of state [15]. A regression curve for the measured points was added by a broken line in the figure for later discussions.

For each temperature, the measured breakdown voltage increases with the density, and its slope changes discontinuously at the points of A<sub>1</sub>, B<sub>1</sub>, and C<sub>1</sub> which are indicated by the closed circle in Fig. 4. The letter symbols, A<sub>x</sub>, B<sub>x</sub>, C<sub>x</sub>, are the same as those used in Fig. 1. At normal temperature, it seems that the broken line in the gas phase consists of a convex upward curve in the low-density region and a convex downward curve in the high-density region. No experiments were done in the region between A<sub>1</sub> and A<sub>2</sub> since the state of medium is a wet vapor of  $\text{CO}_2$ . The average slope in the liquid phase is comparable with that in the gas phase. At near critical and supercritical temperatures, the characteristics in the gas phase are similar to those at normal temperature. The discontinuous points B<sub>1</sub> and C<sub>1</sub> are located near and above the critical

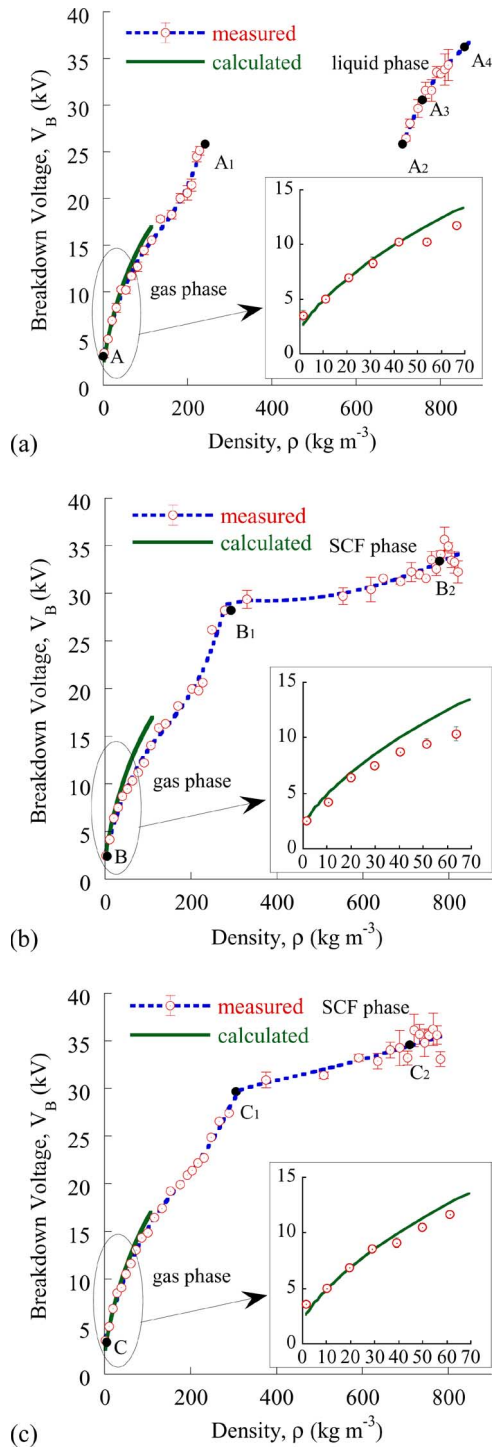


Fig. 4. Breakdown voltage versus density of CO<sub>2</sub> at temperatures of (a) 298 K, (b) 305 K, and (c) 313 K.

pressure in Fig. 1, respectively. The measured average values scatter widely in the higher density region.

2) *Temperature Dependency*: The state of tested medium under a given density changes with the temperature, as shown in Fig. 1. This means that the detailed collision process within CO<sub>2</sub> molecules is affected by the temperature even if the density was kept constant. It is interesting to note the effect of the change in collision process on electrical breakdown mechanism. In order to study this effect from a macroscopic point of

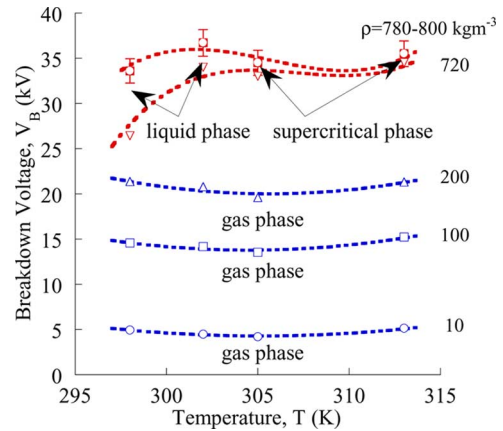


Fig. 5. Temperature dependence of breakdown voltage for five density parameters.

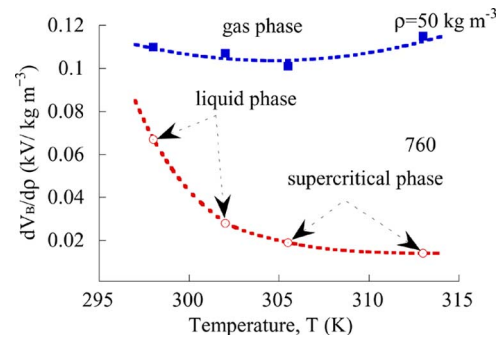


Fig. 6. Temperature dependence of the increasing rate of breakdown voltage for two density parameters.

view, the temperature dependences of breakdown voltage and of the increasing rate of breakdown voltage against the density were investigated.

Taking the density as a parameter, the breakdown voltages from Fig. 4 can be obtained as a function of the temperature, as shown in Fig. 5. In the range of the concerned temperature, the change of the CO<sub>2</sub> state for densities of  $\rho = 10$  to 200, 720, and 780–800  $\text{kg} \cdot \text{m}^{-3}$  are only gas, via lower pressured liquid – higher pressured liquid – supercritical fluid and via higher pressured liquid – supercritical fluid, respectively. The average value and deviation were illustrated by an open circle and vertical bar in the figure since the data are scattered widely in this region.

Fig. 5 shows a remarkable drop in breakdown voltage only at  $\rho = 720 \text{ kg} \cdot \text{m}^{-3}$  at which the state changes from a liquid to the supercritical phase with increasing temperature.

Fig. 6 shows the slope of the breakdown voltage versus density at  $\rho = 50, 760 \text{ kg} \cdot \text{m}^{-3}$ . Clearly, the breakdown rate for the liquid and supercritical phases decreases with temperature but is almost independent of temperature for the gas phase. In particular, remarkable is its change in the temperature region where the state changes from liquid to supercritical phase.

### C. Discussions

1) *Prebreakdown Phenomena in Gas*: It can be argued that the discontinuous points A<sub>1</sub>, B<sub>1</sub>, and C<sub>1</sub> which indicate the

limit of gaseous breakdown voltage characteristics are not necessarily in the gas phase and are located around a position at which the state curve starts to saturate greatly, as shown in Fig. 1. This means that the behavior of a gaseous discharge may be lost when the electron mean free path starts to decrease drastically by a slight increase of pressure.

As stated in Section III-A, the corona onset and breakdown voltages nearly coincide in the gas phase. The measured breakdown voltage is then compared with the theoretical corona onset voltage as follows. According to streamer theory, the corona onset criterion can be given simply by [16]

$$\int \bar{\alpha} dx = K \quad (2)$$

where  $\bar{\alpha}$  is the effective Townsend first ionization coefficient, and  $K$  is the ionization index which is determined empirically by fitting calculated values for a uniform field to the Paschen's curve. The  $\bar{\alpha}$  of CO<sub>2</sub> gas at room temperature can be calculated using

$$\begin{aligned} \frac{\bar{\alpha}}{P} &= 176.5 \exp \left[ -\frac{2.587}{E/P} \right] [1/\text{cm} \cdot \text{kPa}], \\ &\text{for } 0.2 \leq E/P \leq 0.28 [\text{kV/cm} \cdot \text{kPa}] \\ \frac{\bar{\alpha}}{P} &= 50.3 \exp \left[ -\frac{1.515}{E/P} \right] [1/\text{cm} \cdot \text{kPa}], \\ &\text{for } 0.28 < E/P \leq 100 [\text{kV/cm} \cdot \text{kPa}] \end{aligned} \quad (3)$$

where  $P$  is the gas pressure in kPa, and  $E$  is the electric field strength in kV/cm [17], [18]. Equation (3) also can be applied to CO<sub>2</sub> gas at the different temperatures using equivalent gas density which gives the same electron mean free path. The quantitative value of gas density at a given gas temperature and pressure was estimated assuming the tested CO<sub>2</sub> gas as an ideal gas. That is, we modify (3) by introducing the idea of equivalent pressure  $P_e$ , which is given by

$$P_e = \frac{293}{T} P. \quad (4)$$

Then, the gaseous CO<sub>2</sub> at room temperature and pressure  $P_e$  gives the same density as that with pressure  $P$  and temperature  $T$ . Now, we are ready to calculate the corona onset voltage under pressurized conditions using (1) to (4). A constant  $K$  was taken as 20, and the calculated corona onset voltage is shown by a solid line in Fig. 4.

The predicted values are in fairly good agreement with the measured one in the density region of  $\rho = 10\text{--}30 \text{ kg} \cdot \text{m}^{-3}$  with the discrepancy between them increasing with density. However, it is noted that both curves for the measured and estimated breakdown voltage show a convex upward curve in the region of  $\rho = 10\text{--}230 \text{ kg} \cdot \text{m}^{-3}$ . The causes of the discrepancy seem to be that in the higher density region: 1) the experimental conditions are out of the effective region of  $E/P$  for (3); 2) the equation of state for the real gas deviates

from that of an ideal gas; and 3) the gas component changes from pure CO<sub>2</sub> to a mixture of CO<sub>2</sub> molecules and clusters [8], [9].

2) *Breakdown Mechanism in Liquid and Supercritical Liquid:* As stated in Section III-A, corona discharge precedes breakdown in the liquid and supercritical phases, and the corona onset voltage is almost independent of the density. The calculated electric field intensity at the tip of the needle electrode at the corona onset voltage shown in Fig. 3(b) and (c) is on the order of about 450 MV/m which is enough to initiate the field emission. This suggests that corona is triggered by field emission of electrons. That is, all the electrons which are injected from the cathode point collide with CO<sub>2</sub> molecules releasing an instantaneous power density  $W = E \cdot I$ , where  $E$  is the electric field at a specific location around the needle electrode, and  $I$  is the corona or emission current density from the cathode. Due to the different kinds of elastic and inelastic collisions, this power is stored by the CO<sub>2</sub> molecules in different forms: translational energy, rotational, vibrational, and electronic excitation, and ionization energy. The translational and rotational components contribute to an increase in the medium temperature around the cathode electrode. Ionization will occur only at higher fields.

From Fig. 1, the increase in temperature makes the state of CO<sub>2</sub> move horizontally from the original state to the left-hand side of the graph since the pressure was kept constant during the series of breakdown voltage measurements in our experiments. It is interesting to note that the state of the medium after the temperature rise depends on its origin: For the lower pressured liquid, the state changes from liquid to gas, while at higher pressured liquid, the state goes to supercritical. That is, gaseous bubble generation will occur only in the lower pressured liquid. Of course, the state is invariable in the supercritical phase. From the above discussion, the following breakdown mechanism was suggested from the viewpoint of an electrical discharge process: in the liquid and supercritical state, ionization will start with electron emission from the cathode. In the lower pressured liquid, a gaseous bubble is generated due to the power transferred by the emitted electrons. A partial discharge in the bubble will then precede complete breakdown since the dielectric strength is lower than that of the liquid, and the electric field is higher than that in the surrounding liquid due to the greater permittivity of the liquid. In the higher pressured liquid and supercritical fluid, the temperature rise produces a lower density region, and a streamer-type discharge may develop without bubble formation. That is, the bubble-triggered breakdown mechanism will occur only in the lower pressured liquid. This difference in breakdown mechanisms by the experimental conditions may result in the large change in the slope of the breakdown voltage versus density at  $\rho = 760 \text{ kg} \cdot \text{m}^{-3}$  and the remarkable local drop of  $V_B$  at  $T = 298 \text{ K}$  and  $\rho = 720 \text{ kg} \cdot \text{m}^{-3}$  which are shown in Figs. 5 and 6, respectively.

If the proposed breakdown process is true, the breakdown voltage characteristics should change discontinuously near the boundary between the lower and higher pressured liquids. To confirm this, the measured breakdown voltages near the boundary were illustrated in Fig. 7 after magnification of Fig. 4(a).

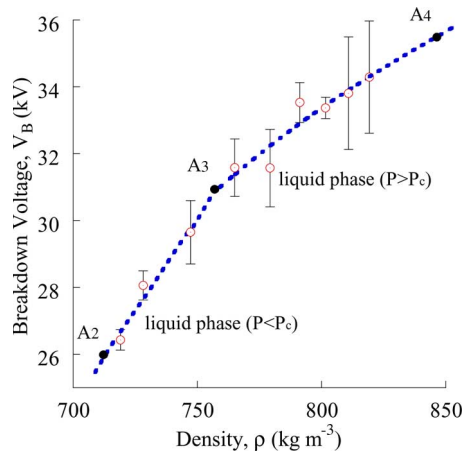


Fig. 7. Detailed illustration of the region of A<sub>2</sub> to A<sub>4</sub> in Fig. 4(a).

As expected, a clear discontinuity appears near the boundary point A<sub>3</sub>.

#### IV. CONCLUSION

The prebreakdown phenomena and breakdown voltage characteristics of a negative dc point-to-plane gap in pressurized CO<sub>2</sub> up to supercritical conditions were investigated experimentally as the first step to develop a plasma reactor with SC CO<sub>2</sub>. The gap length and curvature radius of the point tip were 200 and 30–40 μm, respectively. The obtained results can be summarized as follows.

- 1) Negative corona discharge is unstable in the gas phase, whereas it is stable in liquid and supercritical phases.
- 2) The estimated corona onset voltages by streamer theory are in fairly good agreement with the measured breakdown voltages in the density region of 0.1 to 30 kg · m<sup>-3</sup>, and the discrepancy between them increases with density.
- 3) Gaseous discharge behavior is maintained when the electron mean free path decreases almost linearly with the pressure even if the pressure reaches or exceeds the critical one.
- 4) The characteristics of the breakdown voltage versus density show different behaviors in the medium state: The slope is the largest in the gas phase and decreases with temperature in the liquid and supercritical phases, and the measured breakdown voltage tends to scatter widely in the supercritical and higher density region.
- 5) The breakdown mechanism of the liquid can be classified into two categories: bubble-triggered breakdown in pressures lower than the critical pressure and non bubble-triggered breakdown in pressures higher than the critical pressure.
- 6) The breakdown mechanism in the supercritical phase is similar to that in liquid pressurized higher than the critical pressure: non bubble-triggered breakdown.
- 7) The density and temperature dependences of the breakdown voltage are related to the breakdown mechanism.

It is concluded that if the curvature radius of a higher stressed electrode is smaller than several tenth micrometers, stable corona discharge as a source of cold plasma may be obtained

in liquid and supercritical fluid for a CO<sub>2</sub> plasma reactor. In the discussed experiments, the drastic decrease in breakdown voltage near the critical point [11] was not observed.

The prebreakdown mechanism would be affected by the polarity of the point electrode. We already have some interesting results about the polarity effect. They will be reported elsewhere in the near future since the present paper focused on discharge phenomena in a negative point-to-plane gap. Moreover, detailed study of breakdown mechanism in higher pressurized liquid and supercritical CO<sub>2</sub> based on the electron beam data such as electron collision cross sections of ionization, excitation, and so on would be an interesting research subject in the future.

#### REFERENCES

- [1] K. M. Dooley, C. C. Koa, R. P. Gambrell, and F. C. Knopf, "The use of entrainers in the supercritical extraction of soils contaminated with hazardous organics," *Ind. Eng. Chem. Res.*, vol. 26, no. 10, pp. 2058–2062, 1987.
- [2] G. Madras, C. Erkey, and A. Akgerman, "Supercritical fluid extraction of organic contaminants from soil combined with adsorption onto activated carbon," *Environ. Prog.*, vol. 13, no. 1, pp. 45–50, 1994.
- [3] B. C. Roy, M. Goto, and T. Hirose, "Extraction of ginger oil with supercritical carbon dioxide: Experiments and modeling," *Ind. Eng. Chem. Res.*, vol. 35, no. 2, pp. 607–612, 1996.
- [4] G. Brunner, "Supercritical fluids: Technology and application to food processing," *J. Food Eng.*, vol. 67, no. 1/2, pp. 21–33, 2005.
- [5] U. Topal, M. Sasaki, M. Goto, and K. Hayakawa, "Extraction of lycopene from tomato skin with supercritical carbon dioxide: Effect of operating conditions and solubility analysis," *J. Agric. Food Chem.*, vol. 54, no. 15, pp. 5604–5610, 2006.
- [6] J. Pettersen, A. Hafner, G. Skaugen, and H. Rekstad, "Development of compact heat exchangers for CO<sub>2</sub> air-conditioning systems," *Int. J. Refrig.*, vol. 21, no. 3, pp. 180–193, 1998.
- [7] M. H. Kim, J. Pettersen, and C. W. Bullard, "Fundamental process and system design issues in CO<sub>2</sub> vapor compression systems," *Prog. Energy Combust. Sci.*, vol. 30, no. 2, pp. 119–174, 2004.
- [8] M. A. McHugh and V. J. Kruckonis, *Supercritical Fluid Extraction: Principles and Practice*, 2nd ed. Boston, MA: Butterworth-Heinemann, 1994.
- [9] Y. Arai, T. Sako, and Y. Takebayashij, *Supercritical Fluids. Molecular Interactions, Physical Properties, and New Applications*. Berlin, Germany: Springer-Verlag, 2002.
- [10] R. Hackam and H. Akiyama, "Air pollution control by electrical discharges," *IEEE Trans. Dielectr. Electr. Insul.*, vol. 7, no. 5, pp. 654–683, Oct. 2000.
- [11] T. Ito and K. Terashima, "Generation of micrometer-scale discharge in supercritical fluid environment," *Appl. Phys. Lett.*, vol. 80, no. 16, pp. 2854–2856, Apr. 2002.
- [12] T. Ito, H. Fujiwara, and K. Terashima, "Decrease of breakdown voltages for micrometer-scale gap electrodes for carbon dioxide near the critical point: Temperature and pressure dependencies," *J. Appl. Phys.*, vol. 94, no. 8, pp. 5411–5413, 2003.
- [13] E. H. Lock, A. V. Saveliev, and L. A. Kennedy, "Initiation of pulsed corona discharge under supercritical conditions," *IEEE Trans. Plasma Sci.*, vol. 33, no. 2, pp. 850–853, Apr. 2005.
- [14] S. L. Philp, "Compressed gas insulation in the million-volt range: A comparison of SF<sub>6</sub> with N<sub>2</sub> and CO<sub>2</sub>," *IEEE Trans. Power App. Syst.*, vol. PAS-82, no. 66, pp. 356–359, Jun. 1963.
- [15] R. Span and W. Wagner, "A new equation of state for carbon dioxide covering the fluid region from the triple point temperature to 1100 K at pressure up to 800 MPa," *J. Phys. Chem. Ref. Data*, vol. 25, no. 6, pp. 1509–1596, Nov. 1996.
- [16] A. Pedersen, "Calculation of spark breakdown voltage or corona starting voltage in nonuniform fields," *IEEE Trans. Power App. Syst.*, vol. 86, no. 2, pp. 200–206, Feb. 1967.
- [17] A. Rein, "Breakdown mechanisms and breakdown criteria in gases: Measurement of discharge parameters, a literature survey," *Electra*, no. 32, pp. 43–60, 1974.
- [18] N. H. Malik and A. H. Qureshi, "Breakdown gradient in SF<sub>6</sub> – N<sub>2</sub>, SF<sub>6</sub> – Air, and SF<sub>6</sub> – CO<sub>2</sub> mixtures," *IEEE Trans. Electr. Insul.*, vol. EI-15, no. 5, pp. 413–418, Oct. 1980.



**Tsuyoshi Kiyan** (M'07) was born in Okinawa, Japan, in 1965. He received the B.S. degree from University of the Ryukyus, Okinawa, Japan, in 1996 and the M.S. and Dr. Sci. degrees from Kumamoto University, Kumamoto, Japan, in 1998 and 2002, respectively.

He is currently a Research Associate with the 21st Century Center of Excellence Program on Pulsed Power Science, Kumamoto University.



**Akihiro Uemura** was born in Fukuoka, Japan, in 1982. He received the B.S. degree from Kumamoto University, Kumamoto, Japan, in 2005, where he is currently pursuing the M.S. degree.



**Bhupesh C. Roy** was born in Bangladesh in 1957. He obtained the B.Sc. and M.Sc. degrees from the Department of Applied Chemistry and Chemical Technology, Rajshahi University, Bangladesh, in 1980 and 1981, respectively, and the Ph.D. degree in supercritical fluids extraction technology (chemical engineering) from Kumamoto University, Kumamoto, Japan, in 1996.

He is an Associate Professor of Chemical Engineering in the Department of Applied Chemistry and Chemical Technology, Islamic University, Kushtia,

Bangladesh. On deputation, since 2003, he has been with 21st Century Center of Excellence Program on Pulsed Power Science, Kumamoto University, as a Research Associate. His research interest includes supercritical carbon dioxide extraction from natural sources and in the generation of discharges in supercritical fluids, including their industrial uses.



**Takao Namihira** (M'00–SM'05) was born in Shizuoka, Japan, on January 23, 1975. He received the B.S., M.S., and Ph.D. degrees from Kumamoto University, Kumamoto, Japan, in 1997, 1999, and 2003, respectively.

From 1999 to 2006, he was a Research Associate at Kumamoto University, where he is currently an Associate Professor. During 2003–2004, he was on sabbatical leave at the Center for Pulsed Power and Power Electronics, Texas Tech University, Lubbock.



**Masanori Hara** (M'79–SM'89–F'06) was born in Kagawa, Japan, in 1942. He received the B.S. degree from Kyushu Institute of Technology, Fukuoka, Japan, in 1967 and the M.S. and Dr. Eng. degrees from Kyushu University, Fukuoka, in 1969 and 1972, respectively.

Since 1986, he has been a Professor in the Department of Electrical and Electronic Systems Engineering, Kyushu University, and has been engaged in research on electric power engineering, HV pulsed power engineering, superconductivity, and applied electrostatics. He retired from Kyushu University in 2006. Currently, he is an Emeritus Professor of Kyushu University, an Invited Professor of Kumamoto University, Kumamoto, Japan, and an Advisor of Research Laboratory, Kyushu Electric Company, Inc., Japan.

Dr. Hara was a Vice-President of the Institute of Electrical Engineers, Japan, and President of the Institute of Engineers on Electrical Discharges, Japan.



**Mitsuru Sasaki** was born in Iwate, Japan, on May 31, 1972. He graduated from the Graduate School of Chemical Engineering, Tohoku University, Sendai, Japan, where he received the Ph.D. degree in 2000.

He was with the Genesis Research Institute, Inc., Nagoya, Japan, as a Researcher for developing a new biomass upgrading process with supercritical water during 2000–2003. Since 2003, he has been with Kumamoto University, Kumamoto, Japan, as a Research Associate during 2003–2005 and as an Associate Professor during 2005–present.



**Motonobu Goto** was born in Aichi, Japan, on August 7, 1956. He received the Ph.D. degree from Nagoya University, Nagoya, Japan, in 1984.

He was a Research Associate at Nagoya University from 1984 to 1988. He joined the faculty at Kumamoto University, Kumamoto, Japan, from 1988, where he is currently a Professor in the Department of Applied Chemistry and Biochemistry. He studied at University of California, Davis, as a Visiting Researcher from 1988 to 1990.

Dr. Goto was awarded by The Society of Chemical Engineers Japan in 2006, by Japan Society for Food Engineering in 2004, and by The Japan Society of Adsorption in 1995.



**Hidenori Akiyama** (M'87–SM'99–F'00) received the M.S. and Ph.D. degrees from Nagoya University, Nagoya, Japan, in 1976 and 1979, respectively.

From 1979 to 1985, he was a Research Associate at Nagoya University. In 1985, he joined the faculty at Kumamoto University, Kumamoto, Japan, where he is currently a Professor.

Dr. Akiyama received the IEEE Major Education Innovation Award in 2000 and the IEEE Peter Haas Award in 2003.